PAPER

Check for updates

Synthesis and characterization of novel poly cysteine methacrylate nanoparticles and their morphology and size studies†

Yaseen G. Kareem,[ab] Shwan Rachid[d] and O. Al-Jaf [ID] *[c]

Polymer nanoparticles (PNPs) have significantly advanced the field of biomedicine, showcasing the remarkable potential for precise drug delivery, administration of nutraceuticals, diagnostics/imaging applications, and the fabrication of biocompatible materials, among other uses. Despite these promising developments, the invention faces notable challenges related to biodegradability, bioactivity, target-site specificity, particle size, carrier efficiency, and controlled release. Addressing these concerns is essential for optimizing the functionality and impact of PNPs in biomedical applications. Here, new poly cysteine methacrylate nanoparticles (PCMANPs), *ca.* (200 nm) in size have been synthesized from the cysteine methacrylate (CysMA) monomer using different strategies, including emulsion and inverse emulsion polymerization techniques. The monomer was synthesized using the Michael addition reaction, involving the addition of 3-(acryloyloxy)-2-hydroxypropyl methacrylate to the sulfhydryl group (−SH) of the cysteine (Cys) active site, with the aid of dimethyl phenyl phosphine (DMPP) as a nucleophilic agent as previously reported. To enhance nano-polymerization, a thorough exploration of various initiators, including ammonium persulfate (APS) and 4,4′-azobis (4-cyanovaleric acid) (ACVA), alongside surfactants, such as polyvinyl alcohol (PVA), polyvinyl pyrrolidone (PVP), and sodium dodecyl sulfate (SDS), was conducted. Additionally, critical parameters, such as reaction time, temperature, and solvents, were systematically investigated due to their substantial influence on the shape, size, stability, and morphology of the synthesized polymer nanoparticles. This comprehensive approach aims to optimize the synthesis process, ensuring precise control over the key characteristics of the resulting nanoparticles for enhanced performance in diverse applications. Various characterization techniques, including field emission scanning electron microscopy (FESEM), transmission electron microscopy (TEM), nuclear magnetic resonance (NMR), Raman spectroscopy, Fourier-transform infrared spectroscopy (FTIR), zeta potential, and zeta sizer dynamic light scattering (DLS) analysis, were utilized to investigate purity, morphology, and particle size of the PNPs. As a result, a spherical, monodispersed (homogenized), and stable PCMANP with defined size and morphology was achieved. This may exhibit a remarkable achievement in the future of drug delivery systems and therapeutic index.

Introduction

The inherent complexity of some specific diseases, including cancer and side effects or toxicity associated with their treatment systems increasingly demand a new strategy for drug

[a]*Charmo Center for Research, Training, and Consultancy, Charmo University, Chamchamal, Kurdistan Region, 46023, Iraq*

[b]*Medical Laboratory Science, Komar University for Science and Technology, Sulaymaniah, Kurdistan Region, 46001, Iraq*

[c]*Department of Applied Chemistry, College of Science, Charmo University, Chamchamal, Kurdistan Region, 46023, Iraq. E-mail: omed.ameen@chu.edu.iq*

[d]*Department of Medical Laboratory Science, College of Science, Charmo University, Chamchamal, Kurdistan Region, 46023, Iraq*

† Electronic supplementary information (ESI) available: Characterisation techniques RAMAN, FTIR, and NMRs, for both monomer (CysMA) and polymer (PCMANP). See DOI: https://doi.org/10.1039/d4ra00067f

delivery systems (DDS).[1–3] The main therapeutic goals of such systems are to transport the drug through the body, not only to improve its efficacy but also to ensure its mobility, safety, and security, along with suitable drug loading and timely release, at the site of action and across the paths in biological membranes.[2] Thus, the strategy of DDS includes the drug administration route and different vectors to enhance drug application and diffusion through the human body. Consequently, DDS have become increasingly reliable systems to tackle issues related to therapeutic efficacy, mobility, safety, and active ingredients to target specific sites of action, compared to classic routes.[4]

Based on the previously described characteristics of nano DDS, researchers have assessed various materials as precursors of nanocarriers and techniques for the improvement of DDS applicability; better results have been achieved with such

systems. Due to their excellent biocompatibility, biodegradability and non-immunogenicity, polymer molecules are becoming of great relevance in nanotechnology, in general, and they are particularly being used as NP precursors for DDS. In addition, polymer molecules are a unique material that may feature all above-mentioned characteristics while offering great synthetic versatility. These characteristics have encouraged researchers to use them for end results, such as DDS.[3,5] In general, polymer molecules can be involved in building DDS *via* two different strategies. First, DDS could be obtained directly from biopolymers by chemical derivatization. Second, synthesis of DDS from corresponding monomers is possible, which can lead to a large range of DDS structures and applications.[1,6]

Generally, as a structure, two types of polymeric nanoparticles are targeted: nanospheres and nanocapsules. Nanospheres are matrix particles, solid in nature, with the capability to adsorb compounds at their surface or encapsulate them. Nanocapsules, on the other hand, have a vesicular shape, resembling containers with a liquid core enveloped by solid substances. The entrapped materials are confined within a liquid core cavity, surrounded by a solid shell.[7] Spherical nanocapsules are made of synthetic polymers, such as polyesters (PLGA, PLA, PGA, and poly(hydroxybutyrate-*co*-valerate) (PHBV)), poly (alkyl cyanoacrylate), polyanhydrides, and various block copolymers. These materials have been extensively explored for encapsulation purposes, including delivery of drugs[8] and growth factors.[9,10]

Amino acids serve as fundamental building blocks for polypeptides and proteins in nature. They are extensively functionalized by the optical activity of their side chains. These monomers are recognized for their distinct catalytic behaviors, chirality, and biodegradability, which can be conveyed onto surfaces made from them. Polymers that result from sequences of amino acid side chains possess optical activity, pH sensitivity, biocompatibility, and unique structural and self-assembly properties.[11] These inherent qualities have driven scientists to explore the application of amino acids in various areas, including the synthesis of polymer brushes[12] for application in biomaterials and nanotechnology.[13] Amino acids are also employed in the synthesis of poly-amino acids for drug delivery as nano drug carriers in the field of nanomedicine,[14–16] as protein carriers,[17] and in green chemistry.[18]

The monomer, amino acid methacrylate, was initially studied by Kulkarni and Morawetz, who synthesized amino acid (meth)acrylamides without using protecting group chemistry; they reacted (meth)acryloyl chloride with amino acids.[19] Methionine-based zwitterionic methacryloyl sulfonium sulfonate monomer was prepared by Tanmoy et al.[20] Similarly, certain amino acids exhibit free radical polymerization. Morcellet et al. explored this phenomenon with L-alanine, glutamic acid, aspartic acid, asparagine, phenylalanine, and glycylglycine-based methacrylamides to investigate the impact of chirality on the solution, aggregation, and metal-complexing properties of resulting amino acid-functional vinyl polymers.[21–28] Additionally, Endo and co-workers examined the optical activity and assembly of poly(meth)acrylamides based on individual amino acids, such as L-leucine, L-phenylalanine, L-

glutamic acid, L-tyrosine, methionine, proline, and cysteine.[29–38] Furthermore, serine and serine di, and tri-polypeptides were synthesized by North et al.[39–42]

Due to the rapid coupling of the sulfhydryl group (–SH) with methacrylate derivatives through the Thia-Michael addition, L-cysteine was chosen as one of the most effective amino acid side chains to function as the monomeric unit.[11]

This study reports the synthesis of a new polycysteine methacrylate (PCMA) nanoparticle. Various techniques and strategies are used to optimize the conditions of the polymer nanoparticles. Here, we can report spherical, monodispersed (homogenized), and stable polycysteine methacrylate nanoparticles (PCMANPs) with defined size and morphology. Furthermore, due to the composition of its precursors, the polymeric nanoparticle offers biodegradability, biocompatibility, and non-immunogenicity, making it a remarkable achievement in the future of drug delivery systems and the therapeutic index.

Experimental part

Materials and methods

De-ionized water (20 µs cm^{-1}) served as the ambient reaction medium for the synthesis of (CysMA) monomer and was obtained using a distilled water system (Aqua line Ultrafilter).

3-(Acryloyloxy)-2-hydroxypropyl methacrylate (AHPMA), L-cysteine, dimethyl phenyl phosphine (DMPP), and 4,4-azobis(4-cyanopentanoic acid) (ACVA) ≥98% were purchased from Sigma-Aldrich chemicals without additional purification. Additionally, polyvinyl pyrrolidone K-30 (PVP), polyvinyl alcohol (PVA), ethyl acetate 99.0%, dichloromethane (DCM) 99.8%, hydrogen peroxide 30%, sulfuric acid 98%, and dimethyl sulfoxide ≥99.7% (DMSO) were purchased from Biolabo Ltd. Ethanol absolute, dimethyl formamide (DMF) ≥99.5%, and sodium dodecyl sulphate >99% were purchased from MERCK, Carl Roth, Merck-Schuchardt, Germany.

All glassware was cleaned aggressively using Piranha Solution (with a ratio of 7 : 3 for H_2SO_4 to H_2O_2), followed by 30 minutes each in sonication baths (Professional ultrasonic cleaner mrc) containing deionized water, ethanol, acetone, and deionized water again.

Synthesis and characterization of cysteine methacrylate monomer (CysMA)

The synthesis followed procedures similar to those presented by Ladmiral et al. with some modifications.[11]

A total of 12.57 g, 0.0586 mol AHPMA was added over 25 minutes to a stirred aqueous solution of L-cysteine (6.43 g, 0.053 mol) in 300 mL of deionized water. The solution was stirred for 2 hours to obtain a bilayer solution. After adding the catalyst, (8.5 µL, 5.97×10^{-5} mol DMPP), the resulting clear monolayer mixture was washed with (2 × 50 mL) ethyl acetate and (2 × 50 mL) DCM. The solvent was evaporated under pressure using a rotary evaporator (IKA RV3 eco), followed by overnight freezing under −30 °C using a smeg freezer. The contents were then dried for 103 h using a lyophilization technique (FD-10-MR
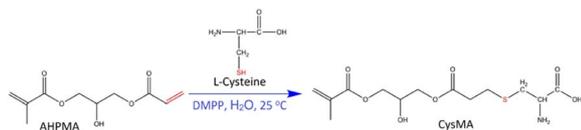
Scheme 1 Synthesis of L-cysteine methacrylate (CysMA) monomers via the Thia-Michael addition.[11]

Freeze Dryer). This process yielded a pure white powder (16.53 g, 87%), as shown in Scheme 1.

¹H NMR (499.36 MHz, DMSO, 298 K) δ (ppm). 1.895 (s, 3H, –CH₃); 2.62, (m, 4H, –S–CH₂–CH₂–COO–); 3.03, (m, 2H, –S–CH₂–CH(COO–)NH₃⁺–); 3.42 (m, 1H, –CHOH); 3.96 (m, 1H, –CH–(COO–)NH₃⁺–); 4.06–4.08 (m, 4H, –CH₂–CHOH–CH₂–); 5.02 (s, 1H, –OH); 5.68 (s, 3H, NH₃); 6.07–6.03 (s, 2H, vinyl) Fig. S1a.†

¹³C NMR (300.8 MHz, DMSO, 298 K) δ (ppm). 18.46 (CH₃–); 26.66 (–S–CH₂–CH₂); 33.03 (–S–CH₂); 34.59 (–S–CH₂–CH₂); 53.77 (–CH₂–CHOH–CH₂–); 65.65–65.80 (2C, –CH₂–CHOH–CH₂–); 66.54 (–CH(COO–) NH₃⁺–); 126.46, 136.21 (2C, vinyl); and 166.87, 169.62, and 171.85 (3C, carbonyls) Fig. S1b.†

Further characterization techniques were applied to confirm the monomer (CysMA) structure. RAMAN and FTIR spectrums (Fig. S2 and S3,† respectively) indicate that the attachment occurred between cysteine (–SH) and AHPMA (C=C) Scheme 1.

Synthesis and optimization of poly cysteine methacrylate nanoparticles (PCMANPs)

We conducted numerous studies to develop suitable polymer nanoparticles, exploring polymerization techniques, ingredient levels, and experimental conditions.

Polymerization techniques. Emulsion and inverse-emulsion polymerization methods were employed to create polymer nanoparticles of various shapes and sizes; agglomerate nanoparticles were obtained as well. In emulsion polymerization, different organic solvents (including ethanol, ethyl acetate, (DCM), (DMF), (DMSO), 1,4-dioxin, and butanol) were tested to dissolve the strongly hydrophilic monomer (CysMA). The study revealed that DMSO and a mixture of ethanol and deionized water (in 4 : 1 ratio) were effective organic solvents to prepare the monomer. The organic phase was introduced dropwise into continuous phases of the aqueous solution of initiators and surfactants. However, DMSO negatively impacted the emulsion formation, while ethanol mixtures led to undesirable traits in the nanoparticles, limiting their application for drug loading.

Due to the strong hydrophilic and poor hydrophobic nature of CysMA, inverse emulsion polymerization was chosen as an alternative technique. In this method, the initiator (ACVA) and surfactant (PVP) were dissolved in DMF to function as the organic phase, which was then mixed with an aqueous solution of CysMA. Ultrasonication was performed for 2 minutes to enhance nano-emulsion nucleation.

Aqueous CysMA (1.5%) was flowed dropwise alongside various concentrations (1.25 to 8.75 mM) of surfactant (2.4 mL) into a stirred solution containing 1.2 mL of organic ACVA solution (0.02 to 0.1 M) over 4 minutes, maintaining a monomer/surfactant flow rate ratio of 4250/600 μL min⁻¹. The

mixture was sonicated for two minutes using an ultrasonication probe (Bandelin Sonoplus probe TT13). The mixture was placed into a pre-heated oil bath reflection system at different temperatures (ranging from 30 to 100 °C) for varying durations (from 15 to 240 minutes). The system was then cooled down, and ethanol was added as an anti-solvent to obtain a milky suspension of poly cysteine methacrylate nanoparticles (PCMANPs). A microcentrifugation apparatus (Thermo Scientific LEGEND Micro 17R) was used to separate the nanoparticles formed. The product thus obtained was washed from all by-products, dissolved in deionized water, and freeze-dried to obtain a pure white precipitate of the PCMANP.

Different techniques were employed for particle characterization, such as field emission scanning electron microscope (FESEM) (MIRA3 TESCAN) and transmission electron microscopy TEM (ZEISS EM10C-100 KV) to observe the nanoparticle morphology in the polymer. Particle size, dispersion stability, and surface charge were confirmed using dynamic light scattering (DLS) and zeta potential measurements (MALVERN ZETASIZER NANO S); surface functional groups of the PCMANPs were analysed using FTIR (Thermo Scientific Nicolet iS 5).

Results and discussion

Synthesis of the cysteine methacrylate (CysMA) monomer

The monomer was prepared through a Thia-Michael addition method as reported formerly, which involves the rapid nucleophilic addition of cysteine sulfhydryl group to the acrylate part of (AHPMA). Dimethyl phenyl phosphine (DMPP) was used as a catalyst, resulting in a strong hydrophilic white powder comprising 85–90% cysteine methacrylate (CysMA) Scheme 1 took place in deionized water within a short reaction period of 2 hours under room temperature conditions. To obtain pure CysMA, the formed monomer mixture was washed with ethyl acetate and (DCM), and the solvent was efficiently evaporated using a rotary evaporator before undergoing freeze drying.[11]

Synthesis of the poly cysteine methacrylate nanoparticles (PCMANPs)

To synthesise the PCMANP with spherical-shaped morphology and particle size on the nanoscale, various polymerization techniques were studied, including emulsion polymerization and inverse emulsion polymerization, which are discussed in following sections.

Emulsion polymerization of CysMA. The emulsion polymerization technique was used to create the desired nano-scale PCMANP.[43] Many parameters, including solvents, surfactants, and initiator ratios, were investigated to improve the configuration and particle size of the polymer nanoparticles. For example, initiators, including APS and ACVA with concentrations of 0.02 M, were examined in an aqueous solution, while SDS was used as a surfactant. The monomers were dissolved in DMSO, but none of them produced efficient results. For example, unexpected particle shapes with a size of about 1.62 μm were obtained from one of the attempts as shown in Fig. 1a.
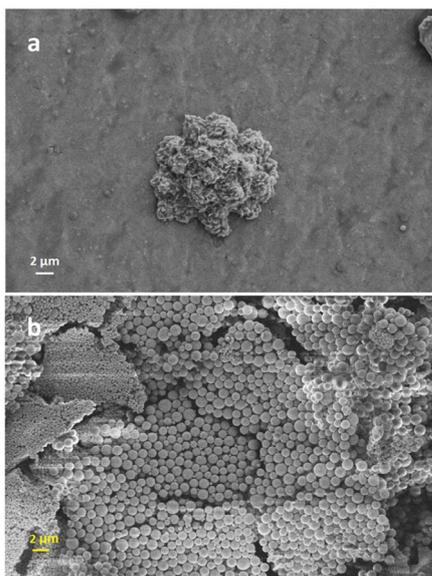
Fig. 1 Polymer micro particles formed with, (a) DMSO used as the organic phase and (SDS 1% 10 mL) and (1.2 mL ACVA 0.02 M) and (b) organic phase (1 : 4 DIW : ethanol), (PVP 1% 10 mL) and (1.2 mL ACVA 0.02 M).

Consequently, we infer that one of the reasons behind the uncontrollable configuration and sizes of the polymer nanoparticles might be the degradation effect of DMSO on the monomer. Another approach was studied that involved dissolving CysMA (1.4%) in a mixture of ethanol and water (4 : 1).

The solution was then slowly introduced into the continuous phase consisting of polyvinylpyrrolidone (PVP) and (ACVA).

The observations revealed that control over the particle morphology and size was poor. For example, inhomogeneous nanoparticles with an average size of around 1.137 μm were achieved as shown in Fig. 1b. As a consequence, to control the shape and size of the polymer nanoparticles, the polymerization technique was switched to inverse emulsion polymerization.

Inverse emulsion polymerization of CysMA. To synthesise the PCMANP from its monomer, inverse emulsion polymerization was used.[44] This method was studied because CysMA is a strong hydrophilic monomer and sparingly soluble in hydrophobic environments. In this method, deionized water (1.5%) served as the continuous phase, while the organic layer formed when surfactant and initiator were dissolved in dimethylformamide (DMF). To control the nano-scale size and morphology of the PCMANP from its monomer, different reaction conditions were investigated. For example, parameters, such as polymerization time, temperature, surfactant, and initiator concentration, were tested. As a result, this technique led to the production of nanoparticles that were more conducive in terms of their shapes and sizes compared to the emulsion polymerization method. The resulting particle sizes and morphology for each study were characterized using field emission scanning electron microscopy (FESEM), transmission electron microscopy (TEM), and dynamic light scattering (DLS) techniques.

Effects of temperature

Preheated oil baths were set to a range of temperatures including, 70, 75, 80, 85, 90, and 95 °C. The influence of polymerization temperatures on the morphology and scale size of the resulting nanoparticles while keeping all other parameters constant were studied using the FESEM technique as shown in Fig. 2a–e, respectively. The results revealed that polymerization initiated at 70 °C (Fig. 2a and Table 1), resulting in the formation of polymer nanoparticles. However, their shape and size were not controlled. The effect of temperatures below 70 °C including 40, 50, and 60 was tested, but the results showed that 70 °C was the threshold, below which there was insufficient nucleation and particle formation. Conversely, at higher temperatures (100 °C), polymer dissolution occurred.

As shown in Fig. 2b and c, the nanoparticles started to form and an optimal polymer was obtained at 85 °C. Above the optimal temperature and precisely at 90 and 95 °C, the morphology of the particle started to deteriorate as illustrated in Fig. 2d and e, respectively and Table 1.

Effects of polymerization duration

After temperature optimization, the duration of the reaction was studied. Prolonged reaction times of 240 min led to the destruction of nanoparticles formed (Fig. 3e). Conversely, when there was insufficient time for nucleation within 30 min of reaction time, no polymer nanoparticles were detected (Fig. 3a)
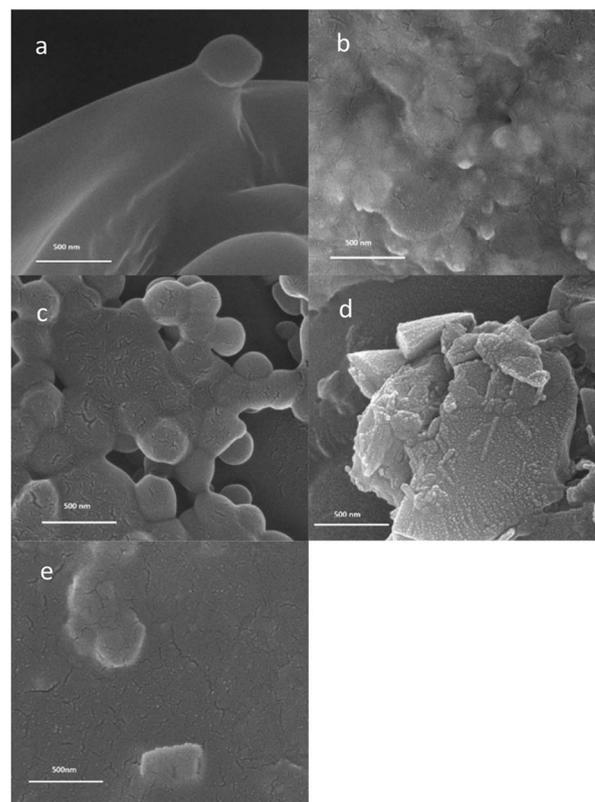

Fig. 2 Effects of temperature on nanoparticles formed: (a) 70 °C, (b) 80 °C, (c) 85 °C, (d) 90 °C and (e) 95 °C mM.

Table 1 Particle size measurements using ImageJ for SEM

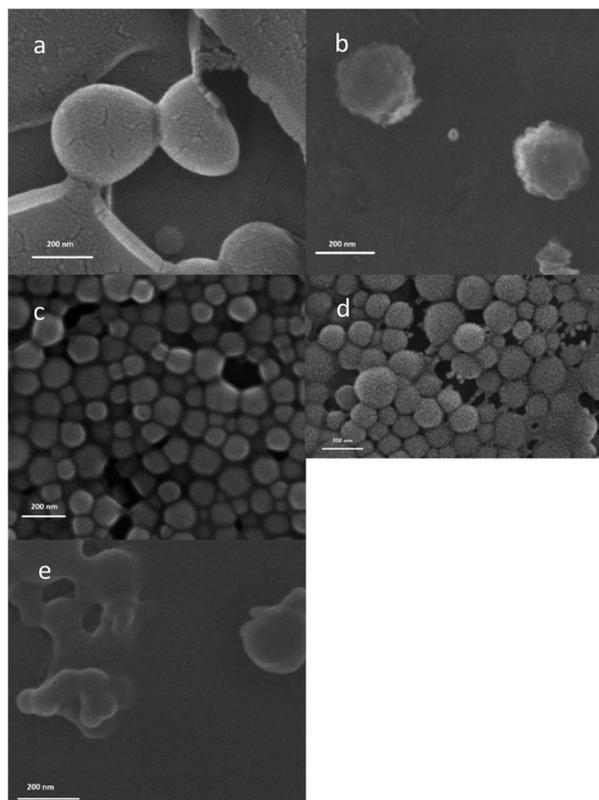| No.	CysMA 1.5% (mL)	PVP (mol)	ACVA (mol L^{-1})	Temp. (°C)	Time (min)	SEM size (nm)	DLS (nm)
1	17	9×10^{-3}	0.02	85	120	226	398.6
2	34	9×10^{-3}	0.02	85	120	267	369.6
3	17	12×10^{-3}	0.02	85	120	110	255.6
4	17	6×10^{-3}	0.02	85	120	184	426.1
5	17	18×10^{-3}	0.02	95	120	84	494.1
6	17	9×10^{-3}	0.02	100	120	127	607.7
7	17	9×10^{-3}	0.02	85	180	140	325.3
8	17	9×10^{-3}	0.02	80	120	156	—

Fig. 3 The effects of polymerization periods on nanoparticles formed, (a) 30 min, (b) 75 min, (c) 120 min, (d) 180 min, and (e) 240 min.

or were poorly formed at 75 min (Fig. 3b). When the duration of polymerization was adjusted at 120 min and 180 min, the most favourable morphology and particle sizes of approximately 110 nm and 140 nm were obtained as shown in Fig. 3c and d, respectively and Table 1.

Effects of initiator levels

To further control the particle size and spherical shape of PCMANP, the effect of different concentrations of ACVA including 0.02, 0.04, 0.06, 0.08, and 0.1 M was investigated, while maintaining the optimum temperature of 85 °C and a reaction period of 120 min. The obtained results clarified that the amount of initiator significantly influenced the

nanoparticle size and morphology. When a concentration of 0.02 M was used, an excellent size of 156 nm was achieved, along with a better spherical shape (Fig. 4a). However, when the concentration increased to 0.04 M, particles started to aggregate due to rapid monomer polymerization (Fig. 4b). In addition, at high concentrations of 0.06, 0.08, and 0.1 M, almost all nanoparticle formation was disturbed, leading to the formation of massive particles (Fig. 4c–e).

Effects of surfactant

After studying the impact of surfactant amount on the PCMANP, we concluded that its effect is significant in this study, even under optimized conditions of other parameters.
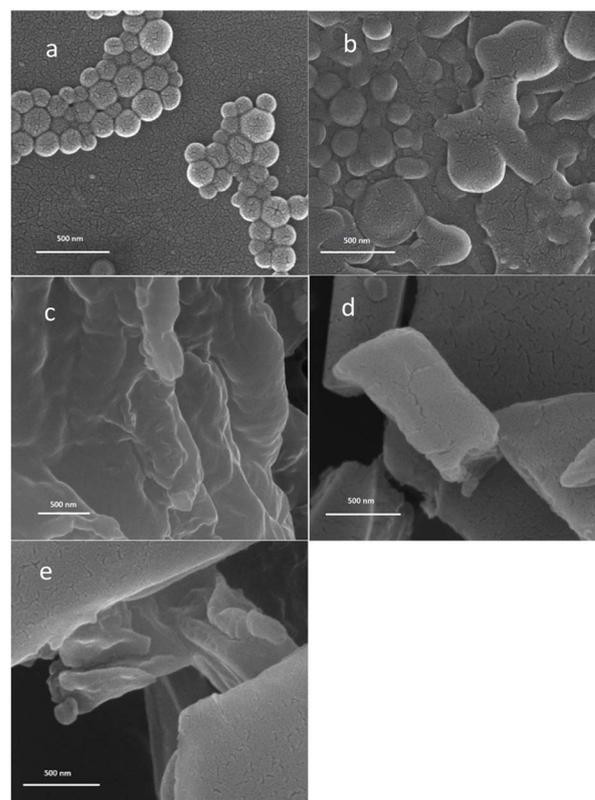

Fig. 4 Effects of initiator (ACVA) concentration: (a) 0.02 M, (b) 0.04 M, (c) 0.06 M, (d) 0.08 M and (e) 0.1 M.

Different surfactant concentrations were tested; 5 mM and 3.75 mM PVP resulted in suitable particle sizes of approximately 110 nm and 156 nm, respectively (Table 1).

As shown in Fig. 5c and d, the PCMANP exhibits effective homogenization, sphericity, and granular shapes. When the concentration decreased to 1.8 mM and 2.5 mM, the particles had no opportunity to complete the nucleation process, resulting in the formation of aggregated nanoparticles, as shown in Fig. 5a and b. When the concentrations of the surfactants increased to 6.25 mM and 8.75 mM, issues started to appear, including disturbed morphology and agglomeration of the nanoparticles, as shown in Fig. 5e and f, respectively and Table 1.

To further explore this aspect of the study, TEM was used, and the results are shown in Fig. 6a–c. The results confirmed that the obtained nanoparticles had a spherical granular morphology and particle size of 210 nm.

Dynamic light scattering (DLS) analysis

To study the surface charge, nanoparticle size, and stability of the PCMANP, we used DLS to measure the polydispersity index (PI) and surface charge of the particles (zeta potential).

Polydispersity index (PI). The polydispersity index (PI) is a dimensionless value that varies with particle sizes in a sample. A lower PI indicates a more monodisperse sample (homogeneous), while a higher PI indicates a more polydisperse sample (heterogeneous).
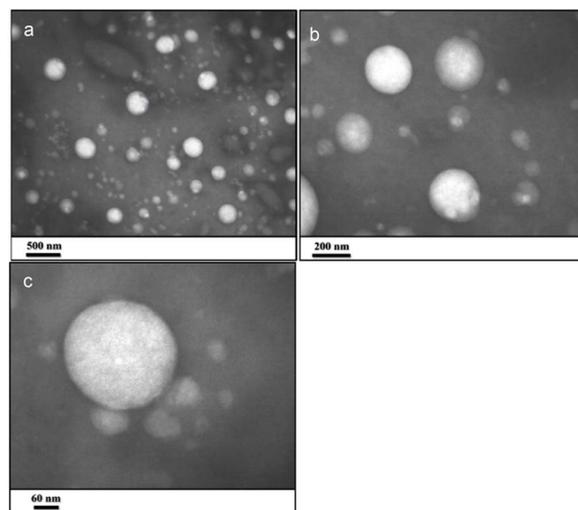

Fig. 5 Effects of PVP concentrations: (a) 1.8 mM, (b) 2.5 mM, (c) 3.75 mM, (d) 5 mM, (e) 6.75 mM and (f) 8.75 mM.

Fig. 6 TEM images of PCMANP confirming particle size and morphology. Scale bars, (a) 500 nm, (b) 200 nm and (c) 60 nm.

• 0 to 0.05: only encountered for monodisperse standard latex or particles.
• 0.05 to 0.08: nearly monodisperse (homogenous) particles.
• 0.08 to 0.7: mid-range polydispersity.
• >0.7: very polydisperse and not suitable for application.

Table 2 clarifies the negative effect of temperature and surfactant concentration on the dispersity index. In the case of an increase in both parameters above their optimum values, the nanoparticles became more heterogeneous (particles of varying sizes) (PI = 1). This could have resulted from the irregular aggregation of the nanoparticles. In contrast, when the duration of polymerization increased to 180 min, suitable monodisperse particles appeared again (particles of similar sizes) (PI = 0.00871).

Zeta potential (ζ). Zeta potential (ζ) is a measure of the electrostatic potential at the slipping plane (also called the shear plane) of particles in a dispersion. This metric typically deals with the stability, charge, and dispersion of the particles. Negative zeta potential values were obtained for all trials and are shown in Table 3. This typically indicates that there is a moderate degree of electrostatic repulsion between particles. This can contribute to the stability of the colloidal system because the particles with similar charges tend to repel each other and stay dispersed in dispersion media. Moreover, the surface charge of the particles dispersed in ethanol is highly negative due to the presence of ionizable groups or functional moieties on particle surfaces.

On the one hand, the value is compatible with RAMAN and FTIR absorbances (1700 and above 3000 cm^{-1}), indicating that nanoparticles possess negative surface charges due to carbonyl and alcoholic functional groups. On the other hand, it is compatible with the polydispersity index (Table 2), as the negative zeta potential can help prevent particle aggregation and flocculation because particles repel each other and tend to maintain a well-dispersed system.
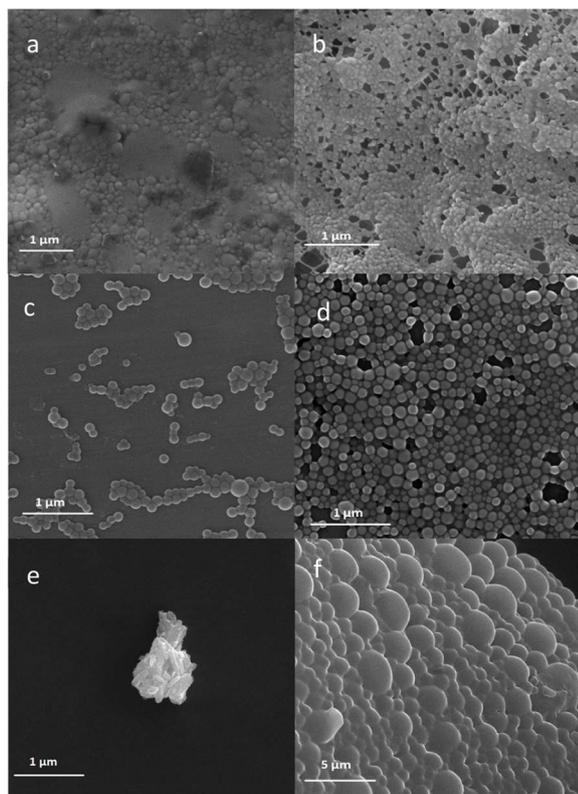
Table 2 Polydispersity index study for optimized parameters

No.	CysMA 1.5% (mL)	PVP (mol)	ACVA (mol L^{-1})	Temp. (°C)	Time (min)	PI	DLS (nm)
1	34	9×10^{-3}	0.02	85	120	0.1812	369.6
2	17	12×10^{-3}	0.02	85	120	0.1192	255.6
3	17	6×10^{-3}	0.02	85	120	0.1754	426.1
4	17	18×10^{-3}	0.02	95	120	1	494.1
5	17	9×10^{-3}	0.02	100	120	1	607.7
6	17	9×10^{-3}	0.02	85	180	0.00871	325.3

Table 3 Zeta potential study for optimized parameters

No.	CysMA 1.5% (mL)	PVP (mol)	ACVA (mol L^{-1})	Temp. (°C)	Time (min)	Zeta potential	DLS (nm)
1	17	9×10^{-3}	0.02	85	120	−19.61	398.6
2	34	9×10^{-3}	0.02	85	120	−19.12	369.6
3	17	12×10^{-3}	0.02	85	120	−12.56	255.6
4	17	6×10^{-3}	0.02	85	120	−11.13	426.1
5	17	18×10^{-3}	0.02	95	120	−14.9	494.1
6	17	9×10^{-3}	0.02	100	120	−20.76	607.7
7	17	9×10^{-3}	0.02	85	180	−19.52	325.3

Conclusion

Cysteine methacrylate (CysMA) monomer was synthesized with an impressive yield of 85–90% in deionized water under normal reaction conditions within a short duration of 2 hours at room temperature. High-quality poly cysteine methacrylate nanoparticles PCMANPs were successfully synthesized with expected average sizes of approximately 200 nm and spherical shape. It was proven that the inverse emulsion polymerization technique provides better polymer nanoparticle configuration and nanoscale size properties compared to emulsion polymerization.

The optimization process involved an accurate study of various parameters, including temperature, time, initiator concentration, and surfactant levels. The morphology, stability, charge, and size of the nanoparticles were precisely characterized using FESEM, TEM and DLS techniques.

The results demonstrated that optimum conditions for nanoparticle formation were achieved at temperatures ranging from 80 to 85 °C, polymerization duration of 120 to 180 minutes, an initiator concentration of 0.02 M, and PVP levels of 3.75 to 5 mM. These conditions yielded monodispersed and homogenized PCMANPs with sizes ranging from approximately 110 to 150 nm. These nanoparticles exhibited excellent stability (as indicated by a polydispersity index of 0.008 to 0.018) and a negative surface charge (with a zeta potential of approximately −20). These findings underscore the effectiveness of the chosen synthesis method and significance of optimizing parameters to tailor the desired properties of the PCMANP. These insights could be a huge step forward in drug delivery system developments in therapeutic fields.

Conflicts of interest

There are no conflicts to declare.

References

1 S. Tran, P.-J. DeGiovanni, B. Piel and P. Rai, *Clin. Transl. Med.*, 2017, **6**, 1–21.

2 W. Xia, Z. Tao, B. Zhu, W. Zhang, C. Liu, S. Chen and M. Song, *Int. J. Mol. Sci.*, 2021, **22**, 9118.

3 B. Begines, T. Ortiz, M. Pérez-Aranda, G. Martínez, M. Merinero, F. Argüelles-Arias and A. Alcudia, *Nanomaterials*, 2020, **10**, 1403.

4 D. Chenthamara, S. Subramaniam, S. G. Ramakrishnan, S. Krishnaswamy, M. M. Essa, F.-H. Lin and M. W. Qoronfleh, *Biomater. Res.*, 2019, **23**, 20.

5 H. K. S. Yadav, A. A. Almokdad, S. I. M. shaluf and M. S. Debe, in *Nanocarriers for Drug Delivery*, ed. S. S. Mohapatra, S. Ranjan, N. Dasgupta, R. K. Mishra and S. Thomas, Elsevier, 2019, pp. 531–556.

6 E. Calzoni, A. Cesaretti, A. Polchi, A. Di Michele, B. Tancini and C. Emiliani, *J. Funct. Biomater.*, 2019, **10**, 4.

7 J. P. Rao and K. E. Geckeler, *Prog. Polym. Sci.*, 2011, **36**, 887–913.

8 M. C. Urbina, S. Zinoveva, T. Miller, C. M. Sabliov, W. T. Monroe and C. S. S. R. Kumar, *J. Phys. Chem. C*, 2008, **112**, 11102–11108.

9 R. R. Sehgal and R. Banerjee, in *Nanomaterials in Tissue Engineering*, ed. A. K. Gaharwar, S. Sant, M. J. Hancock and S. A. Hacking, Woodhead Publishing, 2013, pp. 183–226.

10 S. Zhang and H. Uludağ, *Pharm. Res.*, 2009, **26**, 1561–1580.

11 V. Ladmiral, A. Charlot, M. Semsarilar and S. P. Armes, *Polym. Chem.*, 2015, **6**, 1805–1816.

12 J. Madsen, R. E. Ducker, O. Al Jaf, M. L. Cartron, A. M. Alswieleh, C. H. Smith, C. N. Hunter, S. P. Armes and G. J. Leggett, *Chem. Sci.*, 2018, **9**, 2238–2251.

13 N. Ayres, *Polym. Chem.*, 2010, **1**, 769–777.

14 T. J. Deming, in *Peptide Hybrid Polymers*, ed. H.-A. Klok and H. Schlaad, Springer Berlin Heidelberg, Berlin, Heidelberg, 2006, pp. 1–18.

15 H. Kim, T. Akagi and M. Akashi, *Macromol. Biosci.*, 2009, **9**, 842–848.

16 W. Hu, M. Ying, S. Zhang and J. Wang, *J. Biomed. Nanotechnol.*, 2018, **14**, 1359–1374.

17 T. Akagi, T. Kaneko, T. Kida and M. Akashi, *J. Controlled Release*, 2005, **108**, 226–236.

18 S. Mallakpour and M. Dinari, *J. Macromol. Sci., Part A: Pure Appl.Chem.*, 2011, **48**, 644–679.

19 R. K. Kulkarni and H. Morawetz, *J. Polym. Sci.*, 1961, **54**, 491–503.

20 T. Maji, S. Banerjee, A. Bose and T. K. Mandal, *Polym. Chem.*, 2017, **8**, 3164–3176.

21 C. Methenitis, J. Morcellet-Sauvage and M. Morcellet, *Polym. Bull.*, 1984, **12**, 141–147.

22 C. Methenitis, J. Morcellet-Sauvage and M. Morcellet, *Polym. Bull.*, 1984, **12**, 133–139.

23 A. Lekchiri, J. Morcellet and M. Morcellet, *Macromolecules*, 1987, **20**, 49–53.

24 C. Methenitis, J. Morcellet, G. Pneumatikakis and M. Morcellet, *Macromolecules*, 1994, **27**, 1455–1460.

25 M. Morcellet and C. Loucheux, *Macromolecules*, 1982, **15**, 890–894.

26 J. Morcellet-Sauvage, M. Morcellet and C. Loucheux, *Makromol. Chem.*, 1982, **183**, 831–837.

27 J. Morcellet-Sauvage, M. Morcellet and C. Loucheux, *Makromol. Chem.*, 1982, **183**, 821–829.

28 C. Methenitis, J. Morcellet and M. Morcellet, *Eur. Polym. J.*, 1987, **23**, 287–294.

29 F. Sanda, F. Ogawa and T. Endo, *Polymer*, 1998, **39**, 5543–5547.

30 F. Sanda, T. Abe and T. Endo, *J. Polym. Sci., Part A: Polym. Chem.*, 1997, **35**, 2619–2629.

31 F. Sanda, M. Nakamura and T. Endo, *J. Polym. Sci., Part A: Polym. Chem.*, 1998, **36**, 2681–2690.

32 F. Sanda, M. Nakamura and T. Endo, *Macromolecules*, 1996, **29**, 8064–8068.

33 H. Kudo, F. Sanda and T. Endo, *Macromolecules*, 1999, **32**, 8370–8375.

34 H. Murata, F. Sanda and T. Endo, *Macromolecules*, 1997, **30**, 2902–2906.

35 H. Murata, F. Sanda and T. Endo, *J. Polym. Sci., Part A: Polym. Chem.*, 1998, **36**, 1679–1682.

36 H. Murata, F. Sanda and T. Endo, *Macromolecules*, 1996, **29**, 5535–5538.

37 F. Sanda, J. Kamatani, H. Handa and T. Endo, *Macromolecules*, 1999, **32**, 2490–2494.

38 F. Sanda, M. Nakamura, T. Endo, T. Takata and H. Handa, *Macromolecules*, 1994, **27**, 7928–7929.

39 S. M. Bush and M. North, *Polymer*, 1998, **39**, 933–941.

40 S. M. Bush and M. North, *Polymer*, 1996, **37**, 4649–4652.

41 S. M. Bush, M. North and S. Sellarajah, *Polymer*, 1998, **39**, 2991–2993.

42 A. C. Birchall, S. M. Bush and M. North, *Polymer*, 2001, **42**, 375–389.

43 S. C. Thickett and R. G. Gilbert, *Polymer*, 2007, **48**, 6965–6991.

44 Y. Tamsilian, A. Ramazani S.A., M. Shaban, Sh. Ayatollahi and R. Tomovska, *Colloid Polym. Sci.*, 2016, **294**, 513–525.